Enhancing Thermoelectric Performance of Ternary Nanocrystals through Adjusting Carrier Concentration

Yixin Zhao,[†] Jeffrey S. Dyck,*,[‡] Brett M. Hernandez,[‡] and Clemens Burda*,[†]

Center for Chemical Dynamics and Nanomaterials Research, Department of Chemistry, Case Western Reserve University, 10900 Euclid Avenue, Cleveland, Ohio 44106 and Department of Physics, John Carroll University, 20700 North Park Boulevard, University Heights, Ohio 44118

Received January 1, 2010; E-mail: burda@case.edu; jdyck@jcu.edu

Recently reported nanostructured thermoelectrics have demonstrated improvement in the figure of merit, $ZT = S^2T\sigma/\kappa$,[1] compared to bulk ones by a decrease of thermal conductivity (κ) due to nanoscale grain boundaries and/or an enhancement of the thermopower (S) arising from quantum effects.[2] In these reports, the nanostructures were mostly fabricated by top-down methods, notably by ball milling. Although smaller, more uniform and morphology-controlled thermoelectric nanocrystals (NCs) have been successfully prepared by different chemical approaches, most reported ZT values or power factors ($\sigma*S^2$) of chemically synthesized thermoelectric NCs are not comparable with the values of these top-down prepared thermoelectric NCs or bulk ones.[1] It is found that the relatively lower thermoelectric properties such as lower electrical conductivity σ and/or lower thermopower S are due in large part to inappropriate carrier concentrations. In thermoelectrics, the optimization of carrier concentration is crucial for better thermoelectric performance because the Seebeck coefficient S, electrical conductivity σ, and thermal conductivity κ in the $ZT = S^2T\sigma/\kappa$ are all highly dependent on carrier concentration.[3]

Although the adjustment of carrier concentration is extremely important for the thermoelectric performance, there were very few facile and effective bottom-up methods developed to adjust or optimize the carrier concentration of thermoelectric nanomaterials. One recently reported effective strategy is to adjust the carrier concentrations of PbTe NCs by assembling with Ag_2Te and $PtTe_2$ NCs.[4] This strategy successfully helped improve the carrier concentration and electrical conductivity by several orders of magnitude, but the resulting power factors still need further improvement.

It was already pointed out that an appropriate carrier concentration, above 10^{19} cm^{-3}, is the primary requirement for higher ZT.[5] Recent reported carrier concentrations of chemically synthesized Bi_2Te_3 NCs are of $10^{19}-10^{21}$ cm^{-3}, which are in the appropriate region.[6] However, the corresponding thermoelectric performances are still low because their carrier concentrations still need further optimization. In this report, we adjust the carrier concentration of n-Bi_2Te_3 based NCs by introducing antisite acceptor defects through forming different stoichiometric ternary $Bi_{2-x}Sb_xTe_3$ NCs during the chemical synthesis. The carrier concentrations of these different stoichiometric ratio ternary $Bi_{2-x}Sb_xTe_3$ NCs ($x = 0.02, 0.05, 0.10, 0.20, 0.50$, and 1.5) have been adjusted by a factor of more than 10, and the corresponding power factors are improved three times.

The ternary $Bi_{2-x}Sb_xTe_3$ NCs were synthesized by reacting dodecanethiol coordinated Bi and Sb precursors in stoichiometric ratios $(2 - x)/x$, with freshly prepared trioctylphosphine Te in benzyl ether solution at 150 °C under the protection of Ar gas (detail in the Supporting Information).[7] To achieve better thermoelectric performance, especially electrical conductivity, and to be more convenient for carrier concentration measurement, these $Bi_{2-x}Sb_xTe_3$ NCs were annealed at 380 °C under the protection of Ar, this annealing condition is chosen based on the previous reports and our own TGA experiments (Figure S1).

The XRD patterns of the vacuum-dried and annealed $Bi_{2-x}Sb_xTe_3$ NCs ($x = 0, 0.02, 0.05, 0.10, 0.20, 0.50$, and 1.5) in Figure 1A and B indicate that these $Bi_{2-x}Sb_xTe_3$ NCs with a low partial Sb/Bi substitution level ($x \leq 0.5$) still possess an XRD pattern of Bi_2Te_3 NCs. There is no significantly observable peak shift found in these $Bi_{2-x}Sb_xTe_3$ NCs compared to Bi_2Te_3 NCs because the lattice parameters of Bi_2Te_3 and Sb_2Te_3 are very close. However, when $x = 1.5$, the XRD pattern of $Bi_{0.5}Sb_{1.5}Te_3$ NCs with a high partial Sb/Bi substitution level is consistent with the standard data of $Bi_{0.5}Sb_{1.5}Te_3$ and shows peak shifts compared to Bi_2Te_3 NCs as expected, based on standard data, which indicated the formation of the ternary $Bi_{2-x}Sb_xTe_3$ solid solution. The actual elemental composition of these $Bi_{2-x}Sb_xTe_3$ NCs ($x = 0, 0.02, 0.05, 0.10, 0.20, 0.50$, and 1.5) was analyzed by ICP and listed in Table S1, and the elemental composition of these NCs is close to the nominal composition of the precursor solutions (see Supporting Information). Furthermore, there were no significant X-ray diffraction peaks related to oxidation and impurity phases found in these XRD patterns. The XRD pattern evolution from the vacuum-dried (Figure 1A) to the annealed (Figure 1B) $Bi_{2-x}Sb_xTe_3$ NCs shows the peak intensity increasing and the peak width narrowing after annealing, as expected and similar to previous work.[6]
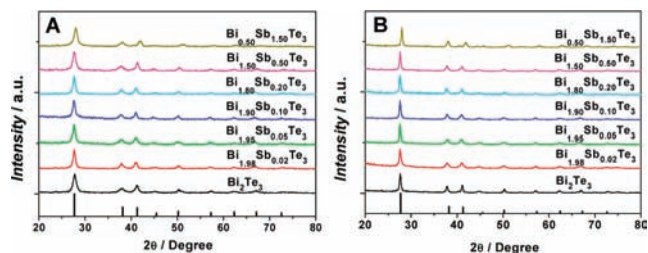

Figure 1. XRD pattern of Sb doped bismuth telluride $Bi_{2-x}Sb_xTe_3$ NCs, vacuum-dried (A) and annealed at 380 °C for 5 h under argon atmosphere (B). The red bars are JCPDS standards for rhombohedral Bi_2Te_3 (72-2036).

The average particle size of the vacuum-dried $Bi_{2-x}Sb_xTe_3$ NCs is ~50 nm as indicated in Figure 2 (and Figure 2S), which is reasonably consistent with an average 30 nm grain size obtained from peak broadening in the XRD pattern according to the Scherrer equation (see Supporting Information). After annealing, the average grain size is 40−50 nm according to XRD peak broadening, despite the fact that some particles grow larger as shown in Figures S4

[†] Case Western Reserve University.
[‡] John Carroll University.

and S5. Since the nanoscale grain sizes are largely preserved, room temperature lattice thermal conductivities are less than 0.8 W m^{1-} K^{-1}, while the value for bulk Bi_2Te_3 is ~1.2 W m^{1-} K^{-1}.

The thermoelectric properties of pressed pellets of annealed $Bi_{2-x}Sb_xTe_3$ NCs are listed in Table 1. The Seebeck coefficient (S) of Bi_2Te_3 NCs is -60.5 μV/K, which is larger than the value for the $Bi_{1.98}Sb_{0.02}Te_3$ NCs, -40.1 μV/K. While, the electrical conductivity (σ) of Bi_2Te_3 NCs is 560 Ohm^{-1} cm^{-1}, which is lower than the 611 Ohm^{-1} cm^{-1} of $Bi_{1.98}Sb_{0.02}Te_3$ NCs. This higher electrical conductivity of $Bi_{1.98}Sb_{0.02}Te_3$ NCs than Bi_2Te_3 NCs is consistent with the corresponding lower Seebeck coefficient value. When $x > 0.02$, Seebeck coefficients of $Bi_{2-x}Sb_xTe_3$ NCs increase with the partial Sb/Bi substitution level x, as shown in Table 1. The negative Seebeck coefficients of ternary $Bi_{2-x}Sb_xTe_3$ ($x \leq 0.5$) NCs indicated that they are all n-type semiconductors, while the Seebeck of $Bi_{0.50}Sb_{1.50}Te_3$ NCs with a high Sb/Bi substitution level became positive, which means that they change to p-type semiconductors. In general, in the given stoichiometric range, the electrical conductivities of ternary $Bi_{2-x}Sb_xTe_3$ NCs decreased with a partial Sb/Bi substitution level, x, as shown in Table 1, and the decrease in electrical conductivities is offset with an increase of Seebeck coefficients.
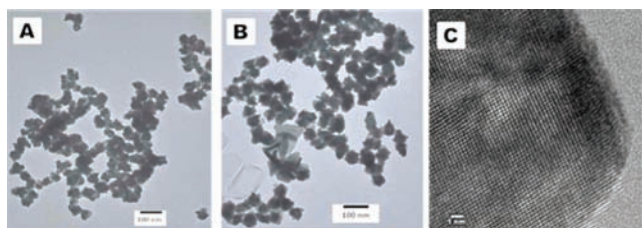

Figure 2. TEM micrographs of vacuum-dried $Bi_{1.80}Sb_{0.20}Te_3$ NCs (A) and $Bi_{0.50}Sb_{1.50}Te_3$ NCs (B) and HRTEM micrograph of vacuum-dried $Bi_{1.50}Sb_{0.50}Te_3$ NCs (C); the scale bar for (A) and (B) is 100 nm, and the scale bar for (C) is 1 nm.

The measured room temperature Hall carrier concentrations of the $Bi_{2-x}Sb_xTe_3$ NCs are listed in Table 1. The carrier concentration of Bi_2Te_3 NCs is 1.96×10^{20} cm^{-3}, and the power factor is 2.08 μW cm^{-1} K^{-2}. Although this value is still much lower than the best bulk value due to its lower electrical conductivity deriving from low carrier mobility,[2] it is already three times higher as the previously reported power factor of chemically synthesized Bi_2Te_3 NCs.[6] At the lowest Sb/Bi substitution level, $x = 0.02$, the carrier concentration increases compared to pure Bi_2Te_3 NCs, which may be due to the increase of possible defects and vacancies introduced. This increase of carrier concentration leads to a decrease of power factor, which is consistent with previous reports.[6] When $x > 0.02$, the carrier concentration of ternary $Bi_{2-x}Sb_xTe_3$ NCs decreases with the partial Sb/Bi substitution level x, and the carrier concentration could be tuned from 2.24×10^{20} to 1.40×10^{19} cm^{-3}. As a result, the power factor ($\sigma*S^2$) of the $Bi_{0.5}Sb_{1.5}Te_3$ NCs is improved three times compared to Bi_2Te_3 NCs, as listed in Table 1. The variation of the power factor with carrier concentration demonstrates (a) that the thermoelectric properties are tuned with adjustment of carrier concentration and (b) that chemical synthesis can play a key role in achieving this.

Here, we propose a plausible mechanism for the tuning of the carrier concentration by partial Sb/Bi substitution. Previous and our chemically prepared Bi_2Te_3 NCs are found to be n-type semiconductors, which could be induced by a possible sulfur impurity or tellurium excess during the chemical synthesis.[6] Second, both Sb and Bi tend to form antisite defects (Bi/Sb on the Te sublattice) resulting in an acceptor role. Because of the closer electron affinity

between Sb and Te than between Bi and Te, a higher Sb content induces additional antisite defects in these ternary $Bi_{2-x}Sb_xTe_3$ NCs.[8] The Sb incorporation thereby reduces the negative carrier concentration by compensating for the background free electrons in the Bi_2Te_3 based NCs which is consistent with the observed carrier concentration trend. These acceptor defects can even convert the $Bi_{2-x}Sb_xTe_3$ NCs from n-type to p-type in the case of $Bi_{0.5}Sb_{1.5}Te_3$ NCs, at very high partial Sb/Bi substitution levels. This behavior is qualitatively the same as that commonly seen in bulk grown crystals.

Table 1. Room Temperature Seebeck Coefficient (S), Electrical Conductivity (σ), Power Factor ($\sigma*S^2$), Carrier Concentration (N) of Annealed $Bi_{2-x}Sb_xTe_3$ NCs

	S (μV/K)	σ (Ohm^{-1} cm^1)	$\sigma*S^2$ (μW cm^{-1} K^{-2})	N (cm^{-3})
Bi_2Te_3	-60.5	560	2.08	1.96×10^{20}
$Bi_{1.98}Sb_{0.02}Te_3$	-40.1	611	0.98	2.24×10^{20}
$Bi_{1.95}Sb_{0.05}Te_3$	-73.7	390	2.12	1.65×10^{20}
$Bi_{1.90}Sb_{0.10}Te_3$	-95.5	286	2.61	1.25×10^{20}
$Bi_{1.80}Sb_{0.20}Te_3$	-126.2	191	3.02	6.20×10^{19}
$Bi_{1.50}Sb_{0.50}Te_3$	-149.0	170	3.78	4.21×10^{19}
$Bi_{0.50}Sb_{1.50}Te_3$	256.6	110	7.21	1.40×10^{19}

In conclusion, we demonstrated an effective method to tune carrier concentrations of n-type Bi_2Te_3 NCs by forming different stoichiometric ternary $Bi_{2-x}Sb_xTe_3$ NCs through chemical partial substitution of Bi with Sb. The carrier concentrations of the ternary $Bi_{2-x}Sb_xTe_3$ NCs were tuned by a factor of more than 10 through different partial Sb/Bi substitution levels. The power factors of ternary $Bi_{2-x}Sb_xTe_3$ NCs were improved more than 3 times with the adjustment of carrier concentrations. Wet chemical alloying is a workable procedure and could become a promising strategy for the adjustment of carrier concentrations of other thermoelectric nanomaterials in the bottom-up synthesis.

Supporting Information Available: Experimental details of synthesis and thermoelectric properties measurement. This material is available free of charge via the Internet at http://pubs.acs.org.

References

(1) (a) DiSalvo, F. J. *Science* **1999**, *285*, 703. (b) Tritt, T. M. *Science* **1999**, *283*, 804.
(2) (a) Poudel, B.; Hao, Q.; Ma, Y.; Lan, Y. C.; Minnich, A.; Yu, B.; Yan, X.; Wang, D. Z.; Muto, A.; Vashaee, D.; Chen, X. Y.; Liu, J. M.; Dresselhaus, M. S.; Chen, G.; Ren, Z. *Science* **2008**, *320*, 63. (b) Minnich, A. J.; Dresselhaus, M. S.; Ren, Z. F.; Chen, G. *Energy Environ. Sci.* **2009**, *2*, 466. (c) Liang, W. J.; Hochbaum, A. I.; Fardy, M.; Rabin, O.; Zhang, M. J.; Yang, P. D. *Nano Lett.* **2009**, *9*, 1689. (d) Wang, R. Y.; Feser, J. P.; Lee, J. S.; Talapin, D. V.; Segalman, R.; Majumdar, A. *Nano Lett.* **2008**, *8*, 2283. (e) Talapin, D. V.; Murray, C. B. *Science* **2005**, *310*, 86.
(3) (a) Dresselhaus, M. S.; Chen, G.; Tang, M. Y.; Yang, R. G.; Lee, H.; Wang, D. Z.; Ren, Z. F.; Fleurial, J. P.; Gogna, P. *Adv. Mater.* **2007**, *19*, 1043. (b) Snyder, G. J.; Toberer, E. S. *Nat. Mater.* **2008**, *7*, 105.
(4) (a) Urban, J. J.; Talapin, D. V.; Shevchenko, E. V.; Kagan, C. R.; Murray, C. B. *Nat. Mater.* **2007**, *6*, 115. (b) Zhou, W. W.; Zhu, J. X.; Li, D.; Hng, H. H.; Boey, F. Y. C.; Ma, J.; Zhang, H.; Yan, Q. Y. *Adv. Mater.* **2009**, *21*, 3196.
(5) Rowe, D. M. *CRC Handbook of Thermoelectrics*; CRC: Boca Raton, FL, 1995.
(6) Dirmyer, M. R.; Martin, J.; Nolas, G. S.; Sen, A.; Badding, J. V. *Small* **2009**, *5*, 933.
(7) (a) Arachchige, I. U.; Kanatzidis, M. G. *Nano Lett.* **2009**, *9*, 1583. (b) Zhao, Y. X.; Burda, C. *ACS Appl. Mater. Interfaces* **2009**, *1*, 1259.
(8) (a) Kavei, G.; Karami, M. A. *Eur. Phys. J. Appl. Phys.* **2008**, *42*, 67. (b) Bludska, J.; Jakubec, I.; Drasar, C.; Lostak, P.; Horak, J. *Philos. Mag.* **2007**, *87*, 325.

JA100020M